

# Flexible PVDF comb transducers for excitation of axisymmetric guided waves in pipe

Thomas R. Hay<sup>\*</sup>, Joseph L. Rose

*ESM Department, Pennsylvania State University, 212 EES Building, University Park, PA 16802, USA*

Received 26 July 2001; received in revised form 21 December 2001; accepted 10 January 2002

## Abstract

Flexible PVDF pipe comb transducers are easy to install by wrapping around any size pipe. It is possible to mechanically couple these transducers to the pipe thereby eliminating the need to bond electrodes to the film and adhesively couple the transducer to the pipe. The simple fabrication process, installation, and affordability of these transducers makes them realistic candidates for condition-based monitoring of some critical pipeline applications. These transducers are capable of exciting lower order axisymmetric modes with minimal radial displacement and maximum axial displacement as well as modes with both surface displacement components. This versatility is extremely important since under certain loading conditions, modes with significant radial displacement are almost completely attenuated. © 2002 Elsevier Science B.V. All rights reserved.

*Keywords:* Axisymmetric guided waves; Comb transducer; PVDF; Pipe

## 1. Introduction

Comb transducers are efficient generators of axisymmetric guided waves in pipe and have many advantages compared to conventional angle beam techniques. Some of these advantages include [1–3] uniform circumferential loading, mode and frequency tuning capability to establish natural defect wave resonances, and higher frequency excitation for improved sensitivity and resolution. Excellent results have been obtained using piezocomposite comb transducers for a variety of different types of defects typically found in piping [4,5]. The flexibility of these transducers is limited by the rigidity of the piezocomposite. Hence, transducer design requires element dicing and other extra manufacturing steps to fit the transducer to the pipe surface.

The flexibility problem can be overcome using PVDF film since this film can be wrapped around and mechanically coupled to the pipe. Earlier results have shown that interdigital transducers using this film as the piezoelectric substrate are efficient generators of the lower order Lamb wave modes in steel and aluminum [6–8] plates. The typical transducer design includes the consideration of a backing layer, electrode pattern and material, electrode bonding to

the PVDF, and bonding the PVDF film to the waveguide. This paper shows that mechanical coupling is an excellent alternative to the bonding steps, thereby simplifying transducer construction and installation.

Pipeline inspection with guided waves is an attractive alternative to conventional bulk wave ultrasonic techniques because it is possible to inspect over long distances and underneath coatings and insulation. Increased sensitivity is also an added advantage but the optimal mode and frequency must be selected such that the wave structure in the pipe cross-section is sensitive to the defect sought in the inspection. In addition, inspection can be complicated by the type of process fluid transported in the pipe and coatings, insulation, and water on the outer surface. As an example, an uncoated and non-insulated natural gas pipeline will typically be less difficult to inspect than a coated pipeline transporting a liquid product. This paper demonstrates that PVDF comb transducers are extremely versatile in exciting modes for both of the above conditions.

## 2. Theoretical background

The derivation of the frequency equation for wave propagation in a hollow isotropic elastic cylinder is given in detail by Gazis [9] and is briefly summarized here. The following forms of the scalar and vector potentials are

<sup>\*</sup> Corresponding author.

*E-mail address:* trh157@psu.edu (T.R. Hay).

assumed:

$$\begin{aligned}\Phi &= f(r) \cos(M\theta) \cos(\omega t + kz), \\ H_r &= g_r(r) \sin(M\theta) \sin(\omega t + kz), \\ H_\theta &= g_\theta(r) \cos(M\theta) \sin(\omega t + kz), \\ H_z &= g_z(r) \sin(M\theta) \cos(\omega t + kz)\end{aligned}\quad (1)$$

where  $\Phi$  is the scalar potential and  $H$  the vector potential. Substituting these equations into the scalar and vector potential wave equations, we get

$$v_1^2 \nabla^2 \Phi = \frac{\partial^2 \Phi}{\partial t^2}, \quad v_2^2 \nabla^2 H = \frac{\partial^2 H}{\partial t^2}\quad (2)$$

where

$$v_1^2 = \frac{\lambda + 2\mu}{\rho}, \quad v_2^2 = \frac{\mu}{\rho}\quad (3)$$

Here  $\lambda$ ,  $\mu$ ,  $\rho$  are the Lamé's constants and density, respectively, we can obtain a general solution for unknown functions  $f(r)$ ,  $g_r(r)$ ,  $g_\theta(r)$ , and  $g_z(r)$  in terms of Bessel and modified Bessel functions. This solution can be used to solve for the displacements fields

$$\begin{aligned}u_r &= \left[ f' + \left( \frac{M}{r} \right) g_3 + k g_1 \right] \cos(M\theta) \cos(\omega t + kz), \\ u_\theta &= \left[ -\left( \frac{M}{r} \right) f + k g_1 + g_3' \right] \sin(M\theta) \cos(\omega t + kz), \\ u_z &= \left[ -k f - g_1' - \frac{(M+1)g_1}{r} \right] \cos(M\theta) \sin(\omega t + kz)\end{aligned}\quad (4)$$

where  $M$  is the circumferential order of the propagating mode and the prime denotes differentiation with respect to  $r$ . The equations for stresses are obtained using the displacement–strain and stress–strain relationships. Using the following boundary conditions  $\sigma_{rr} = \sigma_{rz} = \sigma_{r\theta} = 0$ , at  $r = a$  and  $r = b$ , the frequency equation of the following form is obtained:

$$D = |c_{ij}|\quad (5)$$

where  $c_{ij}$  is a  $6 \times 6$  matrix. For a non-trivial solution, the determinant  $D$  is equal to zero. For axisymmetric longitudinal modes,  $M = 0$ , and the dispersion curves that result from the frequency equation are shown in Fig. 2, where  $fd$  is the frequency thickness product. The thickness refers to the thickness of the cylinder wall. For these modes, the displacement in the circumferential direction  $u_\theta = 0$ , and  $u_r$  and  $u_z$  are the normalized displacement fields for a 35 mm ID and 39 mm OD stainless steel pipe. Examples of displacement fields are shown in Figs. 3 and 8.

### 3. Dispersion curve analysis

Transducer design starts with the analysis of the phase velocity dispersion curves and wave structure. Figs. 1 and 2 show the pipe geometry used and the corresponding phase

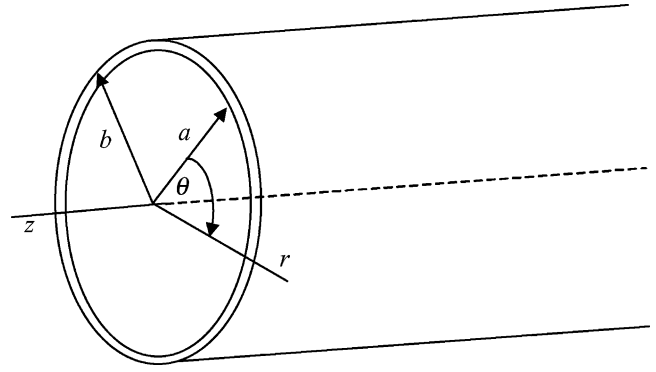


Fig. 1. Pipe coordinates used to model the dispersion curves.

and group velocity dispersion curves, respectively. The design in this paper focused on exciting the  $L(0, 3)$  and  $L(0, 4)$  modes at maximum group velocity to simplify experimental verification and also because both modes have significant particle displacement at both the inner and outer surfaces, demonstrating potential for surface defect detection. In addition, these are points of minimum dispersion which is advantageous for applications that require propagation over long distances. At the bulk wave longitudinal velocity the normal component of the particle velocity of the non-zero-order symmetric Lamb wave modes goes to zero at the free surfaces of a plate [10,11]. Similar results can also be obtained by analyzing the wave structures of the longitudinal axisymmetric modes at the bulk wave longitudinal velocity as shown in Fig. 3. The wave structure shown is normalized to the maximum in-plane displacement component. The out-of-plane and in-plane displacements are represented by the radial and axial components, respectively. At the pipe inner and outer surfaces the axial displacement is maximum while the radial component is close to zero. Consequently,  $L(0, 4)$  is an excellent candidate for inspection of a fluid loaded pipe since coupling of the mode into the fluid will be minimal.

The comb transducer electrodes are activated in phase and are generally separated by a center to center distance of a wavelength. In contrast, interdigital devices typically activate adjacent electrodes with reversed polarity. Both techniques work well but since comb transducers do not require any phase difference between electrodes, the assembly and activation of the transducer are slightly simpler. The wavelength of  $L(0, 4)$  at 5.85 mm/ $\mu$ s is approximately 2.5 mm and was used as the electrode spacing. The wavelength of  $L(0, 3)$  close to the maximum group velocity at a phase velocity of 6.1 mm/ms and an  $fd$  of 1.9 MHz mm was approximately 3.4 mm and was used as the electrode spacing. The activation lines (dotted lines) for the corresponding comb sensors are shown in Fig. 2. This constant wavelength line shows the phase velocities at which the comb transducer will excite each mode while sweeping through frequency. Note that the slope of these lines is given by  $\lambda/d$ , where  $d$  is the pipe thickness.

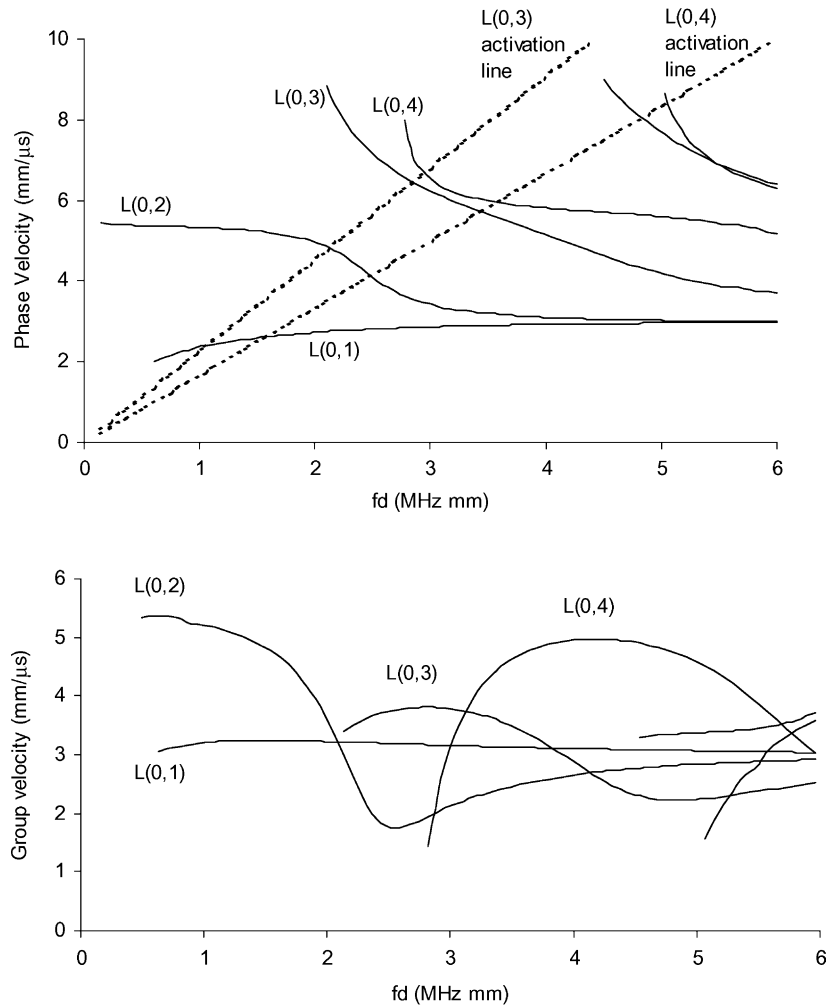


Fig. 2. Phase (top) and group (bottom) velocity dispersion curves for a 35 mm ID and 38 mm OD stainless steel pipe.

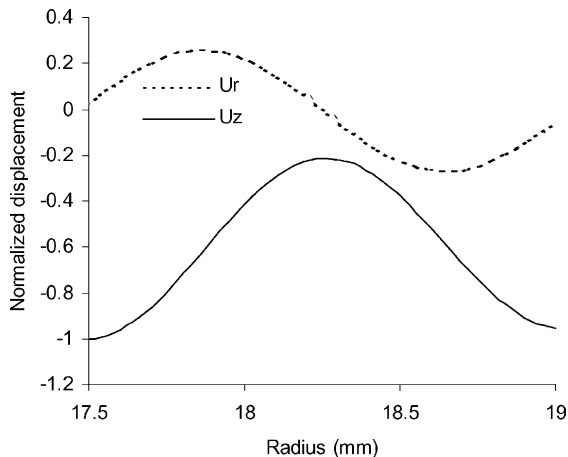


Fig. 3. Normalized L(0, 4) radial ( $u_r$ ) and axial ( $u_z$ ) displacements at the bulk wave phase velocity 5.8 mm/ $\mu$ s and  $fd$  of 3.873 MHz.

#### 4. Transducer fabrication and installation

The objective of the transducer design and fabrication processes was to develop a comb transducer that is easy to

wrap around a pipe, simple to manufacture, and simple to install. As discussed in [6] it can be difficult to deposit metal electrodes onto PVDF. Therefore, bonding an electrode pattern etched on flexible polyamide printed circuit board (PCB) to the PVDF was suggested as an alternative. The fabrication process for the pipe comb transducer used the patterned PCB approach but simplified the process by mechanically coupling the electrodes to the PVDF (Fig. 4). By eliminating the bonding process, the labor associated with the adhesive application and the cost of adhesive material are eliminated. The electrodes were etched onto a polyamide backing using 4 oz. copper. An electrode width of 0.5 mm was used for both designs. The length of the electrodes is 200 mm, which corresponds to the outer circumference of the pipe. Fig. 5 shows the copper finger pattern on the polyamide backing.

The commercially available 100  $\mu$ m thick PVDF film manufactured by Measurement Specialties (MSI) was used as the active element for the transducer. The film was supplied with no electrodes so that the custom electrode patterns could be used on the film. An ammoniacal etching process was used to obtain the desired electrode pattern on

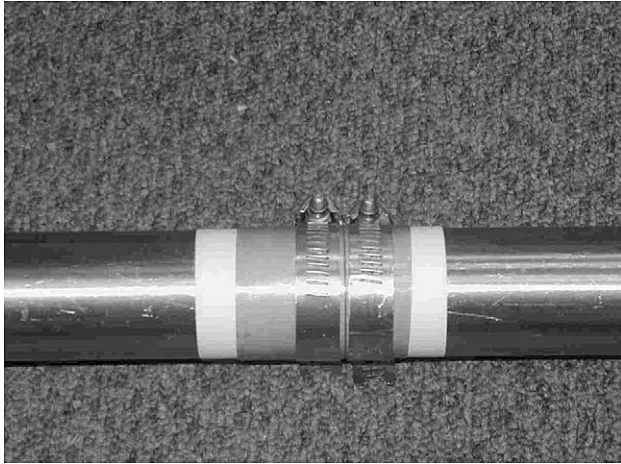


Fig. 4. PVDF comb transducer clamped to a stainless steel pipe.

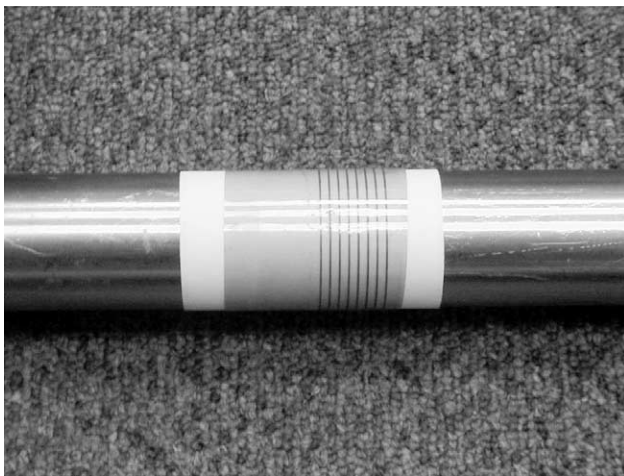


Fig. 5. Electrode finger pattern on flexible polyamide shown wrapped around a pipe.

the 50  $\mu\text{m}$  thick flexible PCB supplied by Armistead Technologies. Since the PVDF wave impedance was small compared to that of the aluminum, the effect of sensor on the surface of the pipe is equivalent to applying stress on the surface [10]. Furthermore, it is assumed that no shear component can be coupled into the specimen and as a result, stress is only applied normal to the outer surface of the pipe. Therefore, both the sending and receiving transducers operate in the thickness mode. Table 1 compares the piezoelectric constants of PVDF and the piezoceramic used in previously developed comb transducers [12].

Table 1  
Piezoelectric stress and strain

Material	$d_{31}$ ( $10^{-12}$ m/V)	$d_{33}$ ( $10^{-12}$ m/V)	$g_{31}$ ( $10^{-12}$ m/V)	$g_{33}$ ( $10^{-12}$ m/V)
PVDF	23	-33	216	-330
PZT-5A	-171	374	-11.4	24.9

The comb was installed by first wrapping the PVDF around the pipe followed by wrapping the electrodes over the PVDF. Pipe clamps were then installed at maximum pressure. No couplant or adhesive was used. The pipe was used as the ground by soldering the transducer's ground electrode to the pipe.

### 5. Experimental setup and results

Experiments were performed using a TISEC structural wave analysis tool (SWAT) system. The system outputs a gated sinusoid in the 50 kHz to 15 MHz frequency range at a maximum voltage of 300 V. The receiver has an output level of 4 V and a dynamic range of 70 dB. For both modes the frequency was swept in the vicinity of the design frequency to maximize the amplitude of the received mode. A pulse width of approximately 11.0  $\mu\text{s}$  was used for both modes and the receiver gain was set to 32 dB for L(0, 3) and L(0, 4). Group velocity measurements were in the through transmission mode at a transducer separation distance of 1800 mm. The attenuation due to water loading was also measured for each mode. Table 2 summarizes the experimental results to demonstrate the importance of mode selection.

Table 2  
Mode group velocity and attenuation

Mode	Operating $fd$ (MHz mm)	Experimental group velocity (mm/ $\mu\text{s}$ )	Water loaded loss (dB)
L(0, 3)	2.8	3.65	31
L(0, 4)	3.7	4.82	5.24

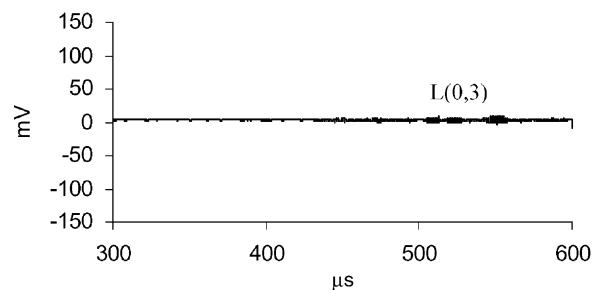
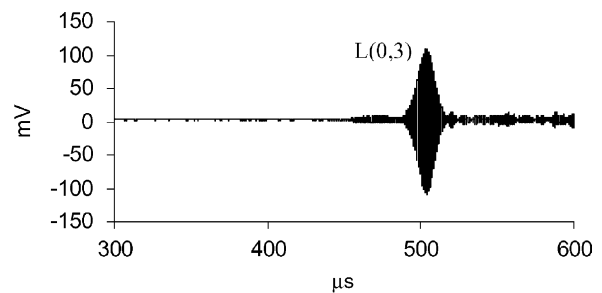


Fig. 6. L(0, 3) at 2.8 MHz mm in a 35 mm ID and 38 mm OD stainless steel pipe (top) and water loaded pipe (bottom).

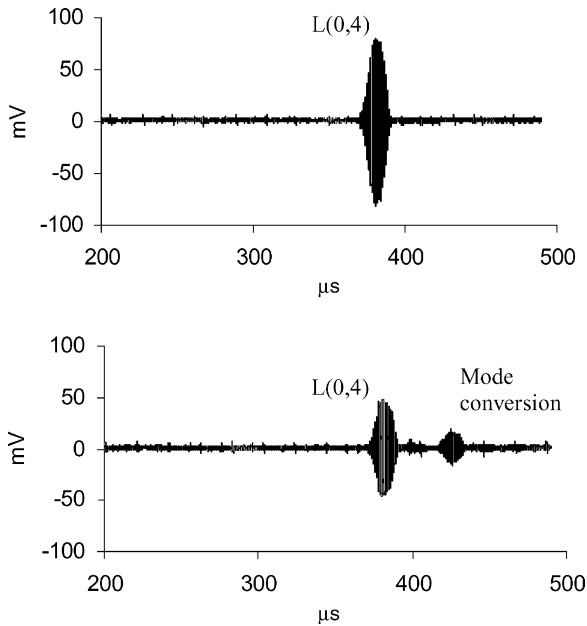


Fig. 7.  $L(0, 4)$  at 3.7 MHz mm in a 35 mm ID and 38 mm OD stainless steel pipe (top) and water loaded pipe (bottom).

For both modes the optimal  $fd$  was found to be slightly lower than that used in the dispersion curve analysis but the group velocities compared excellently. Sample RF waveforms for both modes are provided in Figs. 6 and 7. The out-of-plane surface displacement at the inner radius was also calculated to show the effect of optimizing wave structure for different loading conditions. The comb transducers excite both modes extremely well. The calculated normalized out-of-plane displacement component for the  $L(0, 3)$  mode is shown in Fig. 8. Fig. 3 shows the  $L(0, 3)$  displacement field. The axial/radial displacement ratio for the  $L(0, 3)$  mode is considerably smaller compared to that of the  $L(0, 4)$  mode. As a result, there is a significant difference

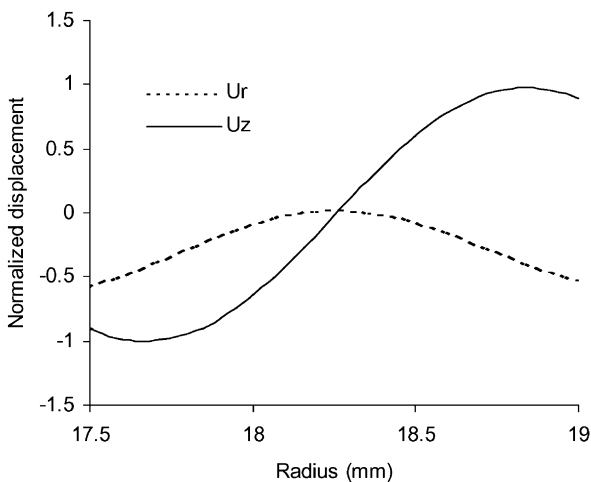


Fig. 8. Wave structure of  $L(0, 3)$  at an  $fd$  of 2.8 MHz mm for a 35 mm ID and 38 mm OD stainless steel pipe.

between the attenuation of the modes due to water loading. The attenuation of the  $L(0, 3)$  mode is almost 25 dB greater than the  $L(0, 4)$  mode. The second waveform in Fig. 7 is a result of mode conversion due to the water loading of the pipe ID.

## 6. Conclusions

The flexible PVDF comb transducers developed in this work successfully excited and received  $L(0, 3)$  and  $L(0, 4)$  close to their maximum group velocities. The design approach focused on affordability and ease of installation. It was shown that no bonding of the PVDF film to the electrodes or test structure was necessary as was done in earlier work. The electrode positioning on the film and transducer installation on the pipe are both performed when the materials are clamped to the pipe. This technique is potentially useful for some long term monitoring applications since issues associated with deterioration of the bond quality or coupling to the pipe are eliminated. It is also feasible to not recover these types of transducers from such applications since the loss of investment is minimal. The wave structure of the excited modes was also considered, showing that the PVDF comb is capable of exciting modes with both strong in-plane and out-of-plane surface displacements. This versatility is extremely important since certain loading conditions on the pipe can significantly attenuate the propagating mode. A comparison of mode propagation in a water loaded pipe was given to demonstrate the importance of mode selection and transducer versatility. It was shown that  $L(0, 3)$  is attenuated approximately 25 dB more than  $L(0, 4)$  at their maximum group velocities over a propagation distance of 1800 mm. The difference in attenuation was due to the relatively weak out-of-plane surface displacement component of  $L(0, 4)$  compared to  $L(0, 3)$ .

## Acknowledgements

The authors would like to thank the Office of Naval Research and Dr. Vinod Agarwala for their support.

## References

- [1] J. Li, J.L. Rose, Implementing guided wave mode control by use of a phased transducer array, *IEEE Trans. Ultrasonics Ferroelectron. Frequency Contr.* 48 (2001) 761–768.
- [2] M.J. Quarry, J.L. Rose, Multimode guided wave inspection of piping using comb transducers, *Mater. Eval.* 45 (1997) 504–508.
- [3] J.L. Rose, Feasibility of ultrasonic guided waves for non-destructive evaluation of gas pipelines, GRI-99/0076, 1999.
- [4] M. Quarry, A time delay comb transducer for guided wave mode tuning in piping, Ph.D. Thesis, Pennsylvania State University, University Park, PA, 2000.

- [5] J.L. Rose, M.J. Quarry, A. Bray, C. Corley, Guided waves for corrosion detection potential in piping under insulation, in: Proceedings of the ASNT Fall Conference, 1997, pp. 27–29.
- [6] R.S.C. Monkhouse, P.D. Wilcox, P. Cawley, Flexible interdigital PVDF Lamb wave transducers for the development of smart structures, *QNDE* 15 (1996) 884–887.
- [7] A. Gachagan, P. Reynolds, G. Hayward, R. Monkhouse, P. Cawley, Piezoelectric materials for application in low profile interdigital transducer designs, in: Proceedings of the IEEE Ultrasonics Symposium, 1997, pp. 1025–1028.
- [8] P.D. Wilcox, M. Castaings, R. Monkhouse, P. Cawley, M.J.S. Lowe, An example of the use of interdigital PVDF transducers to generate and receive a high order Lamb wave mode in a pipe, *QNDE* 16 (1997) 919–926.
- [9] D.C. Gazis, Three-dimensional investigation of the propagation of waves in hollow circular cylinders, *J. Acoust. Soc. Am.* 31 (5) (1959) 568–573.
- [10] I.A. Viktorov, *Rayleigh and Lamb Waves: Physical Theory and Applications*, Plenum Press, New York, 1967, pp. 121–122.
- [11] A. Pilarski, J.J. Ditri, J.L. Rose, Remarks on symmetric Lamb waves with dominant longitudinal displacements, *J. Acoust. Soc. Am. Part I* 4 (1993) 2228–2230.
- [12] G.S. Kino, *Acoustic Wave Devices*, Prentice-Hall, Englewood Cliffs, NJ, 1987.

## Biographies

*Thomas R. Hay* received his BEng from Concordia University in mechanical engineering in 1998 and is currently a PhD candidate in engineering mechanics at Pennsylvania State University. His current research is funded by the Office of Naval Research. Since joining Pennsylvania State's Ultrasonic Non-destructive Evaluation Center he has received the American Society for Non-destructive Testing Fellowship (2000), the National Science and Engineering Research Council of Canada Fellowship (2001–2003), and the Gordon M. MacNabb Scholarship for intelligent systems (2001). His interests include integrating ultrasonic guided wave technology with condition-based maintenance applications.

*Joseph L. Rose (M'74)* is the Paul Morrow Professor in Design and Manufacturing, Department of Engineering Science and Mechanics at Pennsylvania State. He is the author of over 10 patents, four textbooks, and over 350 articles on ultrasonic NDE, wave mechanics, medical ultrasound, adhesive bonding, concrete inspection, pipe and tubing inspection, and composite material inspection. Textbooks include *Basic Physics in Diagnostic Ultrasound* (Wiley, New York, 1979) and *Ultrasonic Waves in Solid Media* (Cambridge University Press, Cambridge, 1999). Current research activity is directed towards wave mechanics, aging aircraft inspection, tubing and piping inspection for the power generation and chemical processing industry, and hidden corrosion detection.